Annals of Nuclear Medicine Vol. 17, No. 3, 205–211, 2003

Preclinical studies on [^{11}C]TMSX for mapping adenosine A_{2A} receptors by positron emission tomography

Kiichi ISHIWATA, Wei-Fang WANG, Yuichi KIMURA, Kazunori KAWAMURA and Kenji ISHII

Positron Medical Center, Tokyo Metropolitan Institute of Gerontology

In previous *in vivo* studies with mice, rats and monkeys, we have demonstrated that [^{11}C]TMSX ([7-methyl-^{11}C]-(*E*)-8-(3,4,5-trimethoxystyryl)-1,3,7-trimethylxanthine) is a potential radioligand for mapping adenosine A_{2A} receptors of the brain by positron emission tomography (PET). In the present study, we performed a preclinical study. A suitable preparation method for [^{11}C]TMSX injection was established. The radiation absorbed-dose by [^{11}C]TMSX in humans estimated from the tissue distribution in mice was low enough for clinical use, and the acute toxicity and mutagenicity of TMSX were not found. The striatal uptake of [^{11}C]TMSX in mice was reduced by pretreatment with theophylline at the dose of 10 and 100 mg/kg, suggesting that the [^{11}C]TMSX PET should be carefully performed in the patients received with theophylline. We have concluded that [^{11}C]TMSX is suitable for mapping adenosine A_{2A} receptors in the human brain by PET.

Key words: Adenosine A_{2A} receptor, [^{11}C]TMSX, central nervous system, positron emission tomography

INTRODUCTION

ADENOSINE is an endogenous modulator of several physiological functions in the central nervous system (CNS) as well as in peripheral organs. The effects are mediated by at least four subtypes: A_1, A_{2A}, A_{2B} and A_3 receptors.[1–3] The adenosine A_1 receptors in the CNS exhibit a higher affinity for adenosine and inhibit adenylyl cyclase, and are present both pre- and post-synaptically in many regions, being rich in the hippocampus, cerebral cortex, thalamic nuclei, basal ganglia and the cerebellar cortex.[4–8] The adenosine A_{2A} receptors exhibit a lower affinity for adenosine, stimulate adenylyl cyclase and are highly enriched in the striatum, nucleus accumbens and olfactory tubercle, in which dopamine D_1 and D_2 receptors are localized at very high densities.[8–10] Both adenosine A_{2A} and dopamine D_2 receptors are co-expressed on GABAergic-enkephaline neurons.[11–14] Therefore, the adenosine A_{2A} receptor can be used as a maker as the dopamine D_2 receptor. However, a number of studies including signal transduction, gene expression, neurotransmitter release and behavioral responses, showed that the adenosine A_{2A} receptors had the opposite effects on dopamine D_2 receptor mediated-effects, although the A_{2A}-D_2 receptor interaction was also suggested.[15]

So far a large numbers of PET and SPECT studies have been performed for charactering degeneration of presynaptic nigrostriatal and post-synaptic striatopallidal neurons of the stratum in the patients with neurological disorders by studying dopaminergic sytem.[16–18] PET targeting the adenosine A_{2A} receptors may be an alternative diagnostic tool. Differential diagnosis of the parkinsonian syndromes such as multiple system atrophy, progressive supranuclear palsy, corticobasal degeneration and diffuse Lewy Body disease is of great interest, because they showed degeneration of post-synaptic as well as presynaptic dopaminergic functions,[11–13] and also because PET and SPECT discriminations among each of the parkinsonian syndromes have been hardly established until now.

Based on the these backgrounds, we have proposed several positron-emitting ligands for mapping the CNS adenosine A_{2A} receptors.[19–26] Among them,

Received December 12, 2002, revision accepted February 14, 2003.

For reprint contact: Kiichi Ishiwata, Ph.D., Positron Medical Center, Tokyo Metropolitan Institute of Gerontology, 1–1 Nakacho, Itabashi-ku, Tokyo 173–0022, JAPAN.

E-mail: ishiwata@pet.tmig.or.jp.

[^{11}C]TMSX[21–23,25] {[7-methyl-^{11}C]-(*E*)-8-(3,4,5-trimethoxystyryl)-1,3,7-trimethylxanthine, Figure 1, abbreviated as [^{11}C]KF18446 previously} and [^{11}C]KF21213[25] {[7-methyl-^{11}C](*E*)-8-(2,3-dimethyl-4-methoxystyryl)-1,3,7-trimethylxanthine} have promising properties as PET ligands.[27] [^{11}C]TMSX has been successfully applied to the imaging of the adenosine A_{2A} receptors in the monkey striatum by PET.[21,22] In a rat model of Huntington's disease, in which quinolinic acid, an excitotoxin, was injected into the striatum to degenerate dopaminergic neurons containing the adenosine A_{2A} receptors, a deceased binding of [^{11}C]TMSX was clearly demonstrated by PET and both *ex vivo* and *in vitro* autoradiographies.[26]

In the present study, we investigated the suitable preparation method for the [^{11}C]TMSX injection, the radiation dosimetry of [^{11}C]TMSX for humans from mice data and the acute toxicity and mutagenicity of TMSX in a preclinical study. We also investigated the effect of theophylline on the [^{11}C]TMSX binding in the brain. Theothylline is widely used as an antasthmatic. Although it has much lower affinity for the adenosine receptors than TMSX, a large dose of theophylline may block partially the binding sites of [^{11}C]TMSX and/or affect the peripheral metabolism of [^{11}C]TMSX, which may change the kinetics in the brain tissue and the plasma radioactivity used as the input function. The stability of the [^{11}C]TMSX injection was also investigated, because *E*-isomer of TMSX analogs having a styryl group in xanthine was isomerized by exposure to visible light to form a stable equilibrium mixture of *E*- and *Z*-isomers, and because the *Z*-isomer is less active than the *E*-isomer.[28]

MATERIALS AND METHODS

(*E*)-1,3-dimethyl-8-(3,4,5-trimethoxystyryl)xanthine and TMSX were synthesized in our laboratory as previously described.[29] Male ddY mice (8-week-old) were obtained from Tokyo Laboratory Animals Co., Ltd. (Tokyo, Japan). The animal studies were approved by the Animal Care and Use Committee of the Tokyo Metropolitan Institute of Gerontology.

Radiosynthesis

[^{11}C]TMSX was prepared by methylation of (*E*)-1,3-dimethyl-8-(3,4,5-trimethoxystyryl)xanthine with [^{11}C]methyl iodide using a previously described method with a slight modification.[22] [^{11}C]CO_2 was produced by the proton irradiation of nitrogen gas at 25 μA for 20 min using the CYPRIS 370 cyclotron (Sumitomo Heavy Industries Ltd., Tokyo, Japan). [^{11}C]Methyl iodide was prepared using an automated synthesis system as previously described,[30] and was trapped in 0.25 m*l* of *N*,*N*-dimethyl formamide containing 0.25 mg of (*E*)-1,3-dimethyl-8-(3,4,5-trimethoxystyryl)xanthine and 5 mg of Cs_2CO_3. The solution was heated at 120°C for 3 min. After adding a mixture of 0.65 m*l* 0.1 M HCl and 0.65 m*l* acetonitrile/water (1/1, v/v), the reaction mixture was applied to the high-performance liquid chromatography (HPLC) to be separated: column, YMC-Pack ODS-A column (10 mm inner diameter (i.d.) × 250 mm length, particle size 5 μm, YMC Co. Ltd., Kyoto, Japan); mobile phase, acetonitrile/water (50/50, v/v); and flow rate, 5 m*l*/min. The [^{11}C]TMSX fraction eluting 6.5–7.0 min was collected in a flask containing 0.05 m*l* of 250 mg/m*l* ascorbate injection and evaporated to dryness. The residue was dissolved in 10 m*l* of physiological saline containing 0.125% (v/v) Tween 80, and the solution was filtered through 0.22 μm membrane filter (Millex GV, Nihon Millipore Ltd., Tokyo, Japan), and stored in an amber glass vial. The radiochemical yield of [^{11}C]TMSX was 2160 ± 330 MBq (range, 1700–2650 MBq) and the specific activity was 71.2 ± 25.9 TBq/mmol (range, 38.4–110 TBq/mmol) at 21–26 min from the end of irradiation (n = 7). The radiochemical purity of [^{11}C]TMSX was >99%, which was determined by HPLC analysis: column, TSKgel super-ODS (4.6 mm i.d. × 100 mm length, particle size 2 μm, Toso Co. Ltd., Tokyo, Japan); mobile phase, acetonitrile/water (40/60, v/v); and flow rate, 1 m*l*/min. All procedures were carried out under dim light to prevent isomerization of the compound.[19,27] The final products included no starting material and no radioactive *Z*-isomer of [^{11}C]TMSX. Finally the sterility and apyrogenicity of the products were confirmed.

Stability of [^{11}C]TMSX

In the other two preparations of [^{11}C]TMSX, the [^{11}C]TMSX fraction was evaporated dryness without ascorbate after HPLC separation, and the [^{11}C]TMSX injection was prepared as described above. Each preparation was stored in a colorless glass vial. Into a preparation 0.05 m*l* of 250 mg/m*l* ascorbate injection was added. These two vials and the amber glass vial containing [^{11}C]TMSX injection prepared were kept under 100 lx visible light at the laboratory, and the radiochemical purity of the three [^{11}C]TMSX preparations was analyzed by HPLC as described above up to 60 min. A portion of the [^{11}C]TMSX with ascorbate in the amber glass vial for injection as prepared above was fractionated into a colorless vial and was exposed to >5000 lx visible light for 60 min.

Tissue distribution in mice

[^{11}C]TMSX (10 MBq/140 pmol) was intravenously injected into mice (8 weeks old). They were killed by cervical dislocation at 1, 5, 15, 30, 60 and 90 min, respectively, after injection (n = 4). The blood was collected by heart puncture, and the tissues were harvested. The samples were measured for the ^{11}C-radioactivity with an auto-gamma counter and weighed. The tissue uptake of ^{11}C was expressed as a percentage of the injected dose per organ (%ID/organ) or a percentage of the injected dose

Table 1 Stability of [^{11}C]TMSX under 100 lx visible light at the laboratory

		Radiochemical purity (%)					
		0 min		30 min		60 min	
		E-isomer	*Z*-isomer	*E*-isomer	*Z*-isomer	*E*-isomer	*Z*-isomer
100 lx visible light							
Amber glass vial	Ascorbate*	>99.9	ND	>99.9	ND	>99.9	ND
Colorless glass vial	Ascorbate**	97.1	ND	95.5	1.6	94.4	3.7
Colorless glass vial	None	97.8	ND	89.0	2.9	85.0	4.6
>5000 lx visible light							
Colorless glass vial	Ascorbate*	>99.9	ND			16.6	83.4

*Ascorbate was added into the [^{11}C]TMSX fractions separated by HPLC before evaporation of dryness, while **it was added into after dissolving the [^{11}C]TMSX evaporated dryness in physiological saline containing 0.125% Tween 80. [^{11}C]TMSX preparations were kept under visible light at 100 lx for 60 min or at >5000 lx for 60 min. ND, not detected.

Table 2 Tissue distribution of radioactivity expressed as a percentage of the injected dose per gram of tissue in mice after intravenous injection of [^{11}C]TMSX

	% Injection dose/g tissue*					
	1 min	5 min	15 min	30 min	60 min	90 min
Blood	1.58 ± 0.33	1.45 ± 0.24	1.29 ± 0.14	1.01 ± 0.20	0.84 ± 0.19	0.95 ± 0.10
Brain	2.49 ± 0.63	2.22 ± 0.11	1.92 ± 0.08	1.61 ± 0.03	1.34 ± 0.07	1.38 ± 0.11
Heart	10.94 ± 1.75	6.59 ± 0.49	5.56 ± 0.74	4.99 ± 0.30	4.29 ± 0.30	4.08 ± 0.60
Lung	3.92 ± 0.95	3.15 ± 0.25	2.53 ± 0.16	2.51 ± 0.22	1.99 ± 0.09	1.96 ± 0.20
Liver	4.42 ± 1.23	9.04 ± 0.86	9.28 ± 0.89	7.97 ± 0.31	7.79 ± 0.72	7.04 ± 0.78
Spleen	2.46 ± 0.91	2.60 ± 0.17	2.27 ± 0.18	2.09 ± 0.19	1.73 ± 0.16	1.67 ± 0.14
Pancreas	4.23 ± 0.88	2.68 ± 0.62	2.80 ± 0.19	2.50 ± 0.06	2.20 ± 0.10	1.92 ± 0.23
Stomach	1.04 ± 0.31	0.77 ± 0.14	0.96 ± 0.23	0.95 ± 0.09	1.26 ± 0.30	1.67 ± 0.27
Small intestine	2.80 ± 0.71	3.65 ± 0.25	4.48 ± 0.26	5.43 ± 0.32	8.41 ± 1.31	9.87 ± 2.19
Large intestine	1.39 ± 0.43	1.79 ± 0.09	2.53 ± 0.29	3.00 ± 0.33	4.32 ± 0.42	7.74 ± 1.17
Kidney	12.08 ± 3.50	9.78 ± 1.47	7.75 ± 0.59	7.17 ± 0.30	6.32 ± 0.38	5.70 ± 1.04
Testis	0.58 ± 0.11	1.21 ± 0.31	1.50 ± 0.15	1.68 ± 0.09	2.35 ± 0.84	1.55 ± 0.31
Bone	1.58 ± 0.17	1.42 ± 0.11	1.25 ± 0.16	1.14 ± 0.15	0.99 ± 0.11	0.95 ± 0.20
Muscle	2.69 ± 0.43	2.16 ± 0.08	1.94 ± 0.06	1.87 ± 0.18	1.53 ± 0.07	1.55 ± 0.32

*Mean ± S.D. (n = 4)

per gram of tissue (%ID/g). Based on the tissue distribution data, radiation dosimetry for human adults was estimated by the MIRD method described previously.[31,32]

Acute toxicity

Toxicity studies were performed at the Mitsubishi Chemical Safety Institute Ltd. (Tokyo, Japan). Acute toxicity was assayed in Crj:CD(SD)IGS rats (SPF). TMSX at a dose of 4.77 mg/kg body weight (0.477 mg/m*l* suspension in physiological saline containing 0.01% Tween 80) was injected intraperitoneally into 5-week old rats weighing 157–168 g and 126–137 g, for males (n = 5) and females (n = 5), respectively. The dose of 4.77 mg/kg body weight is the 37,000-fold equivalent of the postulated administration dose (0.129 μg/kg body weight) of 740 MBq [^{11}C]TMSX with a specific activity of 37 TBq/mmol for humans weighing 60 kg. The three lots of [^{11}C]TMSX prepared above were also assayed after decay-out of ^{11}C. Each of the three [^{11}C]TMSX preparations was injected intravenously into 5-week old male and female rats (n = 3 for each) at doses of 7.07–12.4 μg/3.30–3.93 m*l*/kg body, which were 100-fold equivalent to the postulated administration dose of [^{11}C]TMSX for humans. They were observed four times (0.5, 1, 3 and 6 h after the injection) at day 1 and thereafter once daily for clinical signs until 15 days, and weighed on days 4, 8 and 15. At the end of the 15 day-observation period, the rats were euthanized and a macroscopic analysis was performed.

Ames test

Mutagenicity tests were performed at the Mitsubishi Chemical Safety Institute Ltd. (Tokyo, Japan). TMSX was tested for mutagenicity in the Ames test with four histidine-requiring strains of S*almonella typhimurium* (TA98, TA100, T1535 and T1537) at a dose range of 78.1–5000 μg/plate by the standard method.

Table 3 Organ distribution of radioactivity expressed as a percentage of the injected dose per organ in mice after intravenous injection of [^{11}C]TMSX

	% Injection dose/organ*					
	1 min	5 min	15 min	30 min	60 min	90 min
Brain	1.08 ± 0.25	1.02 ± 0.06	0.88 ± 0.06	0.74 ± 0.09	0.59 ± 0.05	0.61 ± 0.02
Heart	1.60 ± 0.23	1.00 ± 0.08	0.86 ± 0.15	0.78 ± 0.14	0.63 ± 0.05	0.65 ± 0.10
Lung	0.70 ± 0.17	0.56 ± 0.06	0.50 ± 0.04	0.46 ± 0.05	0.44 ± 0.03	0.44 ± 0.02
Liver	9.42 ± 2.30	15.85 ± 2.71	14.66 ± 2.11	14.44 ± 2.51	13.39 ± 0.95	13.72 ± 1.72
Spleen	0.24 ± 0.11	0.29 ± 0.09	0.25 ± 0.05	0.23 ± 0.05	0.20 ± 0.01	0.22 ± 0.09
Pancreas	0.69 ± 0.19	0.44 ± 0.16	0.43 ± 0.10	0.38 ± 0.04	0.31 ± 0.03	0.26 ± 0.04
Stomach	0.98 ± 0.35	0.85 ± 0.05	0.84 ± 0.08	0.92 ± 0.15	0.99 ± 0.09	1.17 ± 0.39
Small intestine	5.79 ± 1.55	7.84 ± 1.25	10.45 ± 0.18	11.80 ± 0.98	13.80 ± 1.57	16.63 ± 3.82
Large intestine	1.32 ± 0.35	1.69 ± 0.08	2.57 ± 0.39	3.30 ± 0.45	4.26 ± 0.66	8.08 ± 2.23
Kidney	6.43 ± 1.64	5.35 ± 0.97	4.41 ± 0.79	3.95 ± 0.54	3.68 ± 0.34	2.90 ± 0.26
Testis	0.13 ± 0.02	0.26 ± 0.09	0.33 ± 0.07	0.36 ± 0.04	0.56 ± 0.19	0.37 ± 0.13
Bladder	0.02 ± 0.01	0.06 ± 0.03	0.08 ± 0.01	0.10 ± 0.04	0.10 ± 0.04	0.11 ± 0.03
Urine	0.01 ± 0.01	0.11 ± 0.05	0.49 ± 0.16	1.09 ± 0.34	3.06 ± 1.54	4.46 ± 1.60

*Mean ± S.D. (n = 4)

Table 4 Absorbed dose of [^{11}C]TMSX for human adults estimated from mouse data

	μGy/MBq		μGy/MBq
Brain	0.09	Upper large intestine wall	3.89
Thyroid	3.95	Lower large intestine wall	3.81
Thymus	4.00	Adrenals	4.92
Breast	3.16	Kidneys	3.62
Heart	0.31	Testis	3.48
Lungs	1.43	Ovaries	4.26
Livers	2.88	Uterus	4.35
Pancreas	2.21	Bladder	2.95
Spleen	2.28	Bone surfaces	3.90
Stomach wall	3.07	Red marrow	3.36
Small intestine wall	4.61	Bones	4.23
	Total body	3.50 μSV/MBq	

Effect of theophylline on the striatal uptake of [^{11}C]TMSX

[^{11}C]TMSX (2.0 MBq/25 pmol) was intravenously injected into mice 15 min after the intraperitoneal injection of theophylline at the doses of 1, 10 and 100 mg/kg, respectively. Fifteen minutes later, the mice were killed by cervical dislocation. The blood and brain were obtained, and the brain was dissected into the striatum, cerebral cortex and cerebellum. The tissue uptake of ^{11}C was expressed as %ID/g.

RESULTS

Stability of [^{11}C]TMSX

Stability of [^{11}C]TMSX was summarized in Table 1. The radiochemical purity of the [^{11}C]TMSX injection containing ascotbate in an amber glass vial remained >99% for 60 min under 100 lx visible light at the laboratory. On the other hand, in a colorless glass vial it lowered with time and *Z*-isomer of [^{11}C]TMSX slightly appeared. At an equilibrium state of [^{11}C]TMSX with ascorbate in a colorless vial by exposure to >5000 lx visible light for 60 min, *E*- and *Z*-isomers were 16.6% and 83.4%, respectively, without no other radioactive impurity.

Radiation dosimetry

The tissue distribution of the radioactivity after injection of [^{11}C]TMSX into mice is summarized in Tables 2 and 3. The highest initial uptake evaluated as %ID/g was found in the kidneys followed by heart, liver, pancreas and lungs. The level of radioactivity in the kidneys, heart, pancreas and lungs gradually decreased. The level in the liver increased for first 15 min and then gradually decreased, whereas those in the small and large intestines increased for 60 min. When the distribution of the radioactivity was evaluated as %ID/organ (Table 3), the uptake was predominant in the liver and small intestine, followed by the kidney and large intestine. The excreted radioactivity as urine was 4.5% of the total injected radioactivity for 90 min. From these data, the radiation-absorbed doses were estimated (Table 4). The radiation-absorbed doses

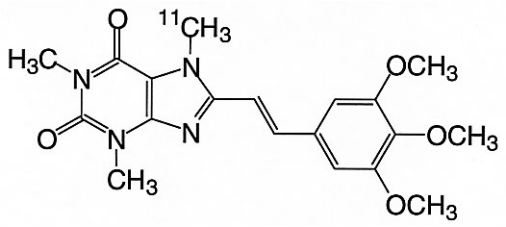

Fig. 1 Chemical structure of [^{11}C]TMSX.

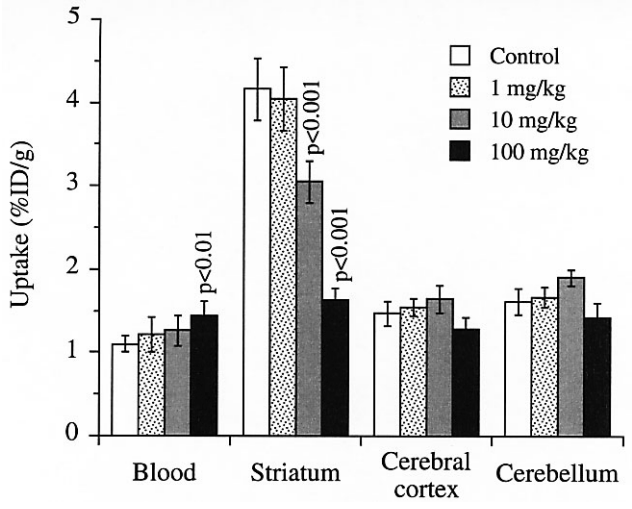

Fig. 2 Effect of pretreatment with theophylline on the regional brain uptake of radioactivity in mice after intravenous injection of [^{11}C]TMSX. Theophylline was intraperitoneally injected into mice at the doses of 1, 10 and 100 mg/kg 15 min before the tracer injection. Mean ± sd (n = 4–5).

were nearly comparable in the organs studied except for the brain and heart.

Acute toxicity

Acute toxicity was evaluated after an intraperitoneally single administration of TMSX at a dose of 4.77 mg/kg, and after an intravenous injection of three lots of [^{11}C]TMSX preparations in a dose range of 3.30–3.93 μg/kg. No mortality was found in the rats. All groups of rats showed normal gain in body weight compared with the control animals, and any no clinical signs were observed over a 15-day period. Also no abnormality was found in their postmortem macroscopic examination.

Mutagenicity

When a bacterial reverse mutation test was conducted on *Salmonella thyphimurium* mutation test, no mutagenic activity was observed for TMSX.

Effect of theophylline on the striatal uptake of [^{11}C]TMSX

As shown in Figure 2, by pretreatment with theophylline at the doses of 10 and 100 mg/kg, the uptake of [^{11}C]TMSX was significantly decreased in the striatum, but not in the cerebral cortex and cerebellum. At the highest dose of theophylline, the blood level of radioactivity was slightly increased.

DISCUSSION

In previous *in vivo* studies on mice, rats, cats and monkeys, we have demonstrated that [^{11}C]TMSX has the potential for mapping adenosine A_{2A} receptors in the CNS.[15–18] In the present work, we investigated the suitable preparation method for the [^{11}C]TMSX injection, the dosimetry of [^{11}C]TMSX and both the acute toxicity and mutagenicity of TMSX as a preclinical study.

Nonaka et al. reported that (*E*)-8-(3,4-dimethoxystyryl)-1,3-dipropyl-7-methylxanthine (KF17837), a TMSX analog, was rapidly isomerized by exposure to visible light to form a stable equilibrium mixture of *E*-isomer (18%) and *Z*-isomer (82%).[28] The *Z*-isomer of KF17837 is much lower affinity for adenosine A_{2A} receptors than the *E*-form: Ki values were 860 nM for *Z*-isomer and 1.0 nM for *E*-isomer (KF17837).[28] In general a styryl group in xanthine derivatives is isomerized and the *Z*-isomers are less active than the *E*-isomer, although the affinity of the *Z*-isomer of TMSX was not investigated. Therefore, we prepared [^{11}C]TMSX injection under dim light to prevent isomerization of a styryl group, and stored it in the presence of ascorbate in an amber glass vial. In these conditions the radiochemical purity of the [^{11}C]TMSX injection was satisfactorily stable. The ascorbate prevented degradation of the [^{11}C]TMSX, but not isomerization.

When the distribution of [^{11}C]TMSX in mice was evaluated as %ID/g, the highest initial uptake was found in the kidneys followed by heart (Table 2). These findings suggest the presence of the specific-binding sites in these organs, because we found previously that [^{11}C]KF17837, an analog of [^{11}C]TMSX, was specifically bound in the heart.[33] A high uptake level in the liver and increasing radioactivity levels in the small and large intestines probably reflect the metabolism of [^{11}C]TMSX in the liver followed by bilary excretion. A high radioactivity level in the kidney and the presence of 4.5% of the total injected radioactivity at 90 min in urine demonstrate that a part of [^{11}C]TMSX and/or its metabolites was also excreted from the kidneys.

The radiation absorbed-doses in organs studied were low enough for clinical use. Neither abnormality in rats in the acute toxicity test nor mutagenecity of TMSX demonstrate the clinical suitability of [^{11}C]TMSX in PET studies of humans.

Clinically theophylline, an adenosine antagonist, is used as an antasthmatic. Its affinities are much lower for the adenosine receptors compared with TMSX; theophylline, Ki = 23000 nM for A_1 receptors and Ki = 16000 nM for A_2 receptors;[29] and TMSX, Ki = 1600 nM for A_1

receptors and Ki = 5.9 nM for A_{2A} receptors.[22,23] Pretreatment with theophylline at the dose of 1 mg/kg did not affect the striatal uptake of [^{11}C]TMSX, whereas larger amounts of the theophylline clearly reduced the striatal uptake of [^{11}C]TMSX. The highest dose of theophylline slightly increased the blood level of radioactivity. This phenomena is probably explained by the blocking of [^{11}C]TMSX binding sites with theophylline in the central and peripheral tissues as described above. Clinical dosage of the theophylline is estimated to be a range of 1–10 mg/kg. Therefore, it is noted that the [^{11}C]TMSX PET should be carefully performed in the patients received theophylline.

In conclusion, these pieces of evidence demonstrated that [^{11}C]TMSX is suitable for mapping adenosine A_{2A} receptors in the human brain by PET.

REFERENCES

1. Fredholm BB, Abbracchio MP, Burnstock G, Daly JW, Harden TK, Jacobson KA, et al. Nomenclature and classification of purinoceptors. *Pharmacol Rev* 1994; 46: 143–156.
2. Haas HL, Selbach O. Functions of neuronal adenosine receptors. *Naunyn Schmiedebergs Arch Pharmacol* 2000; 362: 375–381.
3. Dunwiddie TV, Masino SA. The role and regulation of adenosine in the central nervous system. *Ann Rev Neurosci* 2001; 24: 31–55.
4. Lewis ME, Patel J, Moon Edley S, Marangos PJ. Autoradiographic visualization of rat brain adenosine receptors using N^6-cyclohexyl[^{3}H]adenosine. *Eur J Pharmacol* 1981; 73: 109–110.
5. Goodman RR, Snyder SH. Autoradiographic localization of adenosine receptors in rat brain using [^{3}H]cyclohexyladenosine. *J Neurosci* 1982; 2: 1230–1241.
6. Fastbom J, Pazos A, Palacios JM. The distribution of adenosine A2A receptors and 5′-nucleotidase in the brain of some commonly used experimental animals. *Neuroscience* 1987; 22: 813–826.
7. Fastbom J, Pazos A, Probst A, Palacios JM. Adenosine A2A receptors in the human brain: a quantitative autoradiographic study. *Neuroscience* 1987; 22: 827–839.
8. Svenningsson P, Hall H, Sedvall G, Fredholm BB. Distribution of adenosine receptors in the postmortem human brain: an extended autoradiographic study. *Synapse* 1997; 27: 322–335.
9. Parkinson FE, Fredholm BB. Autoradiographic evidence for G-protein coupled A_2-receptors in rat neostriatum using [^{3}H]-CGS21680 as a ligand. *Naunyn Schmiedebergs Arch Pharmacol* 1990; 342: 85–89.
10. Johansson B, Fredholm B. Further characterization of the binding of the adenosine receptor agonist [^{3}H]CGS 21680 to rat brain using autoradiography. *Neuropharmacology* 1995; 34: 393–403.
11. Gerfen CR, Engber TM, Mahan LC, Susel Z, Chase TN, Monsma FJ, et al. D1 and D2 dopamine receptor-regulated gene expression of strionigral and striopallidal neurons. *Science* 1990; 250: 1429–1432.
12. Schiffmann SN, Jacobs O, Vanderhaeghen JJ. Striatal restricted adenosine A_2 receptor (RDC8) is expressed by enkephalin but not by substance P neurons: an *in situ* hybridization histochemistry study. *J Neurochem* 1991; 57: 1062–1067.
13. Pollack AE, Harrison MB, Wooten GF, Fink JS. Differential localization of A2a adenosine receptor mRNA with D1 and D2 dopamine receptor mRNA in striatal output pathways following a selective lesion of striatonigral neurons. *Brain Res* 1993; 631: 161–166.
14. Augood SJ, Emson PC. Adenosine A_{2a} receptor mRNA is expressed by enkephalin cells but not by somatostatin cells in rat striatum: a co-expression study. *Mol Brain Res* 1994; 22: 204–210.
15. Kase H. New aspects of physiological and pathophysiological functions of adenosine A_{2A} receptor in basal ganglia. *Biosci Biotechnol Biochem* 2001; 65: 1447–1457.
16. Tissingh G, Booij J, Winogrodzka A, van Royen EA, Wolters EC. IBZM- and CIT-SPECT of the dopaminergic system in parkinsonism. *J Neural Transm* 1997; 50 (Suppl): 1–7.
17. Stoessl AJ, Ruth TJ. Neuroreceptor imaging: new developments in PET and SPECT imaging of neuroreceptor binding (including dopamine transporters, vesicle transporters and post synaptic receptor sites). *Curr Opin Neurol* 1998; 11: 327–333.
18. Thobois S, Guillouet S, Broussolle E. Contributions of PET and SPECT to the understanding of the pathophysiology of Parkinson's disease. *Neurophysiol Clin* 2001; 31: 321–340.
19. Ishiwata K, Noguchi J, Toyama H, Sakiyama Y, Koike N, Ishii S, et al. Synthesis and preliminary evaluation of [^{11}C]KF17837, a selective adenosine A_{2A} antagonist. *Appl Radiat Isot* 1996; 47: 507–511.
20. Noguchi J, Ishiwata K, Wakabayashi S, Nariai T, Shumiya S, Ishii S, et al. Evaluation of carbon-11-labeled KF17837: a potential CNS adenosine A_{2a} receptor ligand. *J Nucl Med* 1998; 39: 498–503.
21. Suzuki F, Ishiwata K. Selective adenosine antagonists for mapping central nervous system adenosine receptors with positron emission tomography: Carbon-11 labeled KF15372 (A_1) and KF17837 (A_{2A}). *Drug Develop Res* 1998; 45: 312–323.
22. Ishiwata K, Noguchi J, Wakabayashi S, Shimada J, Ogi N, Nariai T, et al. ^{11}C-labeled KF18446: a potential central nervous system adenosine A_{2a} receptor ligand. *J Nucl Med* 2000; 41; 345–354.
23. Ishiwata K, Ogi N, Shimada J, Nonaka H, Tanaka A, Suzuki F, et al. Further characterization of a CNS adenosine A_{2a} receptor ligand [^{11}C]KF18446 with *in vitro* autoradiography and *in vivo* tissue uptake. *Ann Nucl Med* 2000; 14: 81–89.
24. Ishiwata K, Shimada J, Wang WF, Harakawa H, Ishii S, Kiyosawa M, et al. Evaluation of iodinated and brominated [^{11}C]styrylxanthine derivatives as *in vivo* radioligands mapping adenosine A_{2A} receptor in the central nervous system. *Ann Nucl Med* 2000; 14: 247–253.
25. Wang WF, Ishiwata K, Nonaka H, Ishii S, Kiyosawa M, Shimada J, et al. Carbon-11-labeled KF21213: a highly selective ligand for mapping CNS adenosine A_{2A} receptors with positron emission tomography. *Nucl Med Biol* 2000; 27: 541–546.
26. Ishiwata K, Ogi N, Hayakawa N, Oda K, Nagaoka T,

Toyama H, et al. Adenosine A_{2A} receptor imaging with [^{11}C]KF18446 PET in the rat brain following quinolinic acid lesion: comparison with the dopamine receptor imaging. *Ann Nucl Med* 2002; 16: 467–475.
27. Ishiwata K, Shimada J, Ishii K, Suzuki F. Assessment of adenosine A_{2A} receptors with PET as a new diagnostic tool for neurological disorders. *Drugs Fut* 2002; 27: 569–576.
28. Nonaka Y, Shimada J, Nonaka H, Koike N, Aoki N, Kobayashi H, et al. Photoisomerization of a potent and selective adenosine A_2 antagonist, (*E*)-1,3-dipropyl-8-(3,4-dimethoxystyryl)-7-methylxanthine. *J Med Chem* 1993; 36: 3731–3733.
29. Shimada J, Suzuki F, Nonaka H, Ishii A, Ichikawa S. (*E*)-1,3-dialkyl-7-methyl-8-(3,4,5-trimethoxystyryl)xanthines: potent and selective adenosine A_2 antagonists. *J Med Chem* 1992; 35: 2342–2345.
30. Ishiwata K, Seki H, Ishii K, Ishii S, Nozaki T, Senda M. Synthesis and *in vivo* evaluation of [^{11}C]semotiadil, a benzothiazine calcium antagonist. *Appl Radiat Isot* 1994; 45: 439–443.
31. Ishiwata K, Ido T, Mejia AA, Ichihashi M, Mishima Y. Synthesis and radiation dosimetry of 4-borono-2-[^{18}F]fluoro-D,L-phenylalanine: A target compound for PET and boron neutron capture therapy. *Appl Radiat Isot* 1991; 142: 325–328.
32. Mejia AA, Nakamura T, Itoh M, Hatazawa J, Ishiwata K, Ido T, et al. Absorbed dose estimates in positron emission tomography studies based on the administration of ^{18}F-labeled radiopharmaceuticals. *J Radiat Res* 1991; 32: 243–261.
33. Ishiwata K, Sakiyama Y, Sakiyama T, Shimada J, Toyama H, Oda K, et al. Myocardial adenosine A_{2a} receptor imaging of rabbit by PET with [^{11}C]KF17837. *Ann Nucl Med* 1997; 11: 219–225.